

Review

Multifunctional Aromatic Carboxylic Acids as Versatile Building Blocks for Hydrothermal Design of Coordination Polymers

Jinzhong Gu ^{1,*}, Min Wen ¹, Xiaoxiao Liang ¹, Zifa Shi ¹, Marina V. Kirillova ² and Alexander M. Kirillov ^{2,*}

¹ Key Laboratory of Nonferrous Metal Chemistry and Resources Utilization of Gansu Province, State Key Laboratory of Applied Organic Chemistry and College of Chemistry and Chemical Engineering, Lanzhou University, Lanzhou 730000, China; wenm17@lzu.edu.cn (M.W.); liangxx15@lzu.edu.cn (X.L.); shizf@lzu.edu.cn (Z.S.)

² Centro de Química Estrutural, Instituto Superior Técnico, Universidade de Lisboa, Av. Rovisco Pais, 1049-001 Lisbon, Portugal; kirillova@tecnico.ulisboa.pt

* Correspondence: gujzh@lzu.edu.cn (J.G.); kirillov@tecnico.ulisboa.pt (A.M.K.)

Received: 15 January 2018; Accepted: 29 January 2018; Published: 3 February 2018

Abstract: Selected recent examples of coordination polymers (CPs) or metal-organic frameworks (MOFs) constructed from different multifunctional carboxylic acids with phenyl-pyridine or biphenyl cores have been discussed. Despite being still little explored in crystal engineering research, such types of semi-rigid, thermally stable, multifunctional and versatile carboxylic acid building blocks have become very promising toward the hydrothermal synthesis of metal-organic architectures possessing distinct structural features, topologies, and functional properties. Thus, the main aim of this mini-review has been to motivate further research toward the synthesis and application of coordination polymers assembled from polycarboxylic acids with phenyl-pyridine or biphenyl cores. The importance of different reaction parameters and hydrothermal conditions on the generation and structural types of CPs or MOFs has also been highlighted. The influence of the type of main di- or tricarboxylate ligand, nature of metal node, stoichiometry and molar ratio of reagents, temperature, and presence of auxiliary ligands or templates has been showcased. Selected examples of highly porous or luminescent CPs, compounds with unusual magnetic properties, and frameworks for selective sensing applications have been described.

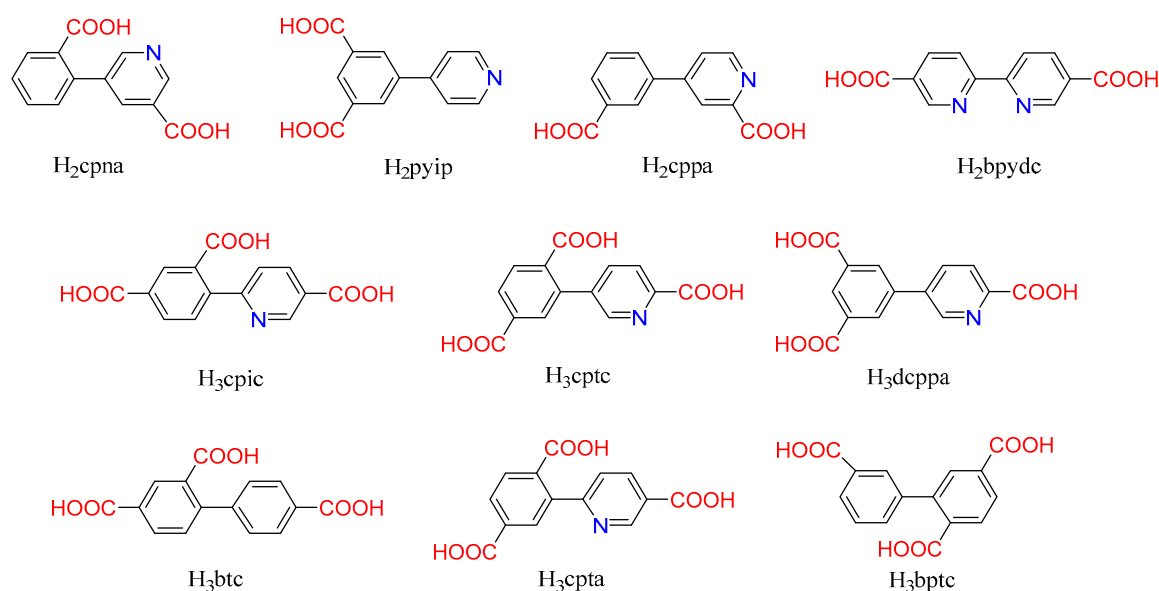
Keywords: coordination polymers; metal-organic frameworks; crystal engineering; hydrothermal synthesis; carboxylic acids

1. Introduction and Scope

In recent years, various crystalline metal-organic architectures (MOAs) including coordination polymers (CPs) or metal-organic frameworks (MOFs) have been an object of very intense research that spans from the fields of crystal design and engineering to chemistry of functional materials [1–15]. In particular, a very interesting research direction concerns the search for new and versatile organic building blocks that can be applied for the design of unusual metal-organic architectures with desirable structural features and notable functional properties [16–19]. Despite considerable progress achieved in this field, the assembly of coordination polymers or metal-organic frameworks in a predictable way is often a difficult task. This is mainly because the assembly of such compounds can depend on various factors, such as the nature and coordination properties of metal nodes [20,21], connectivity and type of organic building blocks [22–24], reaction conditions and stoichiometry [25,26], and effects of templates [27–29] or supporting ligands [30,31].

A high diversity of aromatic polycarboxylic acids has been extensively applied as multifunctional building blocks in designing novel metal-organic networks [32,33]. Among such building blocks, flexible ligands containing biphenyl and phenyl-pyridine cores with a varying number and position of carboxylic groups as well as distinct locations of *N*-pyridyl functionality have attracted a special interest [34,35]. It can be justified by a possibility of two adjacent phenyl and/or pyridine rings to rotate around the C–C single bond and thus conform to a coordination environment of metal nodes. Besides, the presence of several carboxylic groups with a varying degree of deprotonation in addition to an optional *N*-pyridyl functionality can provide multiple and distinct coordination sites, thus leading to different coordination fashions and resulting in the assembly of structurally distinct coordination polymers [36–38]. Furthermore, depending on a deprotonation degree and crystal packing arrangement, these aromatic polycarboxylate ligands can behave as good H-bond acceptors and donors, thus furnishing an extra stabilization of metal-organic structures and facilitating their crystallization.

Hence, the main objective of the present work consists in highlighting selected recent examples of coordination polymers that were hydrothermally assembled from a series of multifunctional carboxylic acids with phenyl-pyridine or biphenyl cores (Scheme 1). These carboxylic acids are still very poorly explored toward the design of CPs or MOFs, but can constitute an interesting type of semi-rigid, thermally stable, multifunctional, and versatile building blocks in crystal engineering research. Thus, the present study briefly discusses the general aspects of hydrothermal synthesis of selected coordination polymers derived from the aromatic carboxylic acids shown in Scheme 1. Some of them represent isomeric biphenyl tricarboxylate blocks (H₃bptc and H₃btc), while other are isomeric phenyl-pyridine tricarboxylate blocks (H₃cpctc, H₃dcppa, and H₃cpta). The study also highlights the influence of various parameters (main ligand type, metal node, molar ratio and stoichiometry, temperature, presence of auxiliary ligand or template) on structural diversity of the obtained products. For selected examples of CPs, functional properties and applications are also highlighted.



Scheme 1. Ten selected multifunctional carboxylic acids used as building blocks for the design of CPs or MOFs.

2. Hydrothermal Synthesis and Structural Diversity of Coordination Polymers

2.1. Advantages of Hydrothermal Synthesis

Hydrothermal synthesis is commonly applied toward the design of metal-organic networks [39–41] and refers to the synthesis and crystallization of coordination compounds that occur under hydrothermal conditions, typically in a hermetically sealed aqueous solution at elevated temperatures and pressures. The hydrothermal synthesis features a number of important advantages over other common methods for preparing CPs, namely: (i) high reactivity of reactants and unique synthetic conditions in terms of a combination of pressures and temperatures; (ii) growth of good quality single crystals (Figure 1) or microcrystalline phases with no need for additional work-up and purification; (iii) possible control of solution or interface reactions, formation of metastable and unique structures that cannot be generated by other methods; (iv) use of water as a green organic-solvent-free reaction medium that can also aid crystallization by supplying labile H₂O ligands to complete coordination environment of metal nodes; and (v) relative simplicity of the equipment.

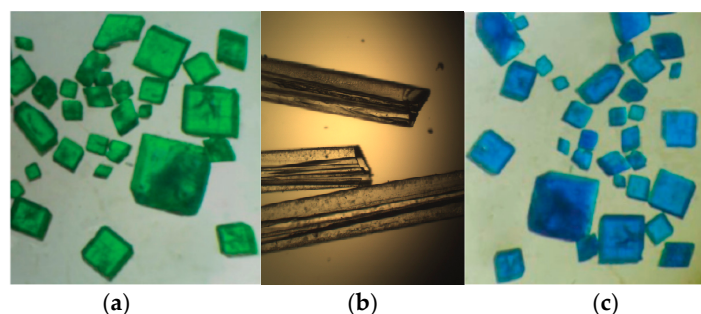


Figure 1. Images showing examples of single crystals of Ni (a), Cd (b), and Cu (c) coordination polymers generated hydrothermally.

For coordination polymers driven by multifunctional carboxylic acids with phenyl-pyridine or biphenyl cores (Scheme 1), typical synthetic procedure begins with mixing, in water at ambient temperature and under constant stirring, a metal nitrate or chloride salt, a main carboxylic acid building block, and an auxiliary ligand (optional) [42–44]. The obtained mixture is then treated with sodium hydroxide as a typical base to adjust the solution pH value in the range of 5–7. Then, the reaction mixture is sealed in a Teflon-lined stainless steel autoclave and subjected to the hydrothermal treatment at 80–210 °C for 2 or 3 days in an oven, followed by gradual cooling to ambient temperature at a rate of 10 °C/h (Figure 2). The autoclaves are opened after being kept at ambient temperature for 24 h. The obtained crystalline solids are filtered off and washed (optional) or isolated manually to furnish a coordination polymer product (Figure 1).



Figure 2. Images of the Teflon-lined stainless steel autoclaves (a) and an oven with temperature control (b) typically applied for the hydrothermal generation of CPs.

2.2. Effect of Building Block Type

The type of the main carboxylic acid ligand (Scheme 1) is one of the structure-defining factors during the hydrothermal synthesis of CPs. Selected examples of different metal-organic networks that were obtained under similar reaction conditions are summarized in Table 1. For example, the use of different dicarboxylic acids (H_2cpna , H_2cppa , or H_2bpydc) as main building blocks and 1,10-phenanthroline as an auxiliary ligand led to the generation of distinct manganese(II) derivatives **1–3** (Figure 3), the structures of which range from a 1D ladder [$Mn(\mu_3-cpna)(phen)(H_2O)_n$] (**1**) and 1D zigzag chain [$Mn(\mu-cppa)(phen)(H_2O)_n$] (**2**) to a 3D MOF [$Mn(\mu_4-bpydc)(phen)_n$] (**3**). The use of a cobalt(II) metal source in combination with the isomeric H_2cpna or H_2cppa ligands and 2,2'-bipyridyl resulted in the assembly of a 2D metal-organic layer [$Co(\mu_3-cpna)(2,2'-bpy)(H_2O)_n$] (**4**) or a 1D zigzag chain {[$Co(\mu-cppa)(2,2'-bpy)(H_2O) \cdot H_2O$]} (**5**). Similar structure-defining influence of tricarboxylic acid building blocks can be observed in other zinc(II) (**6**, **7**) and manganese(II) (**8**, **9**) coordination compounds (Table 1).

Table 1. Selected examples of coordination polymers (CPs) showing an effect of main carboxylate ligand on product structure.

Compound	Formula	Ligand	Structure	Reference
1	$[Mn(\mu_3-cpna)(phen)(H_2O)_n]$	H_2cpna	1D ladder chain	[42]
2	$[Mn(\mu-cppa)(phen)(H_2O)_n]$	H_2cppa	1D zigzag chain	[44]
3	$[Mn(\mu_4-bpydc)(phen)]_n$	H_2bpydc	3D MOF	[45]
4	$[Co(\mu_3-cpna)(2,2'-bpy)(H_2O)_n]$	H_2cpna	2D layer	[42]
5	{[$Co(\mu-cppa)(2,2'-bpy)(H_2O) \cdot H_2O$]} _n	H_2cppa	1D zigzag chain	[44]
6	$[Zn_3(\mu_3-cptc)_2(H_2O)_6]_n$	H_3cptc	1D ladder chain	[46]
7	{[$Zn_3(\mu_5-dcppa)_2(H_2O)_4 \cdot 2H_2O$]} _n	H_3dcppa	3D MOF	[47]
8	$[Mn(\mu-Hdcppa)(phen)(H_2O)_2 \cdot 2H_2O]$	H_3dcppa	0D dimer	[47]
9	{[$Mn(\mu_4-Hcpta)(phen)] \cdot 4H_2O$]} _n	H_3cpta	3D MOF	[48]

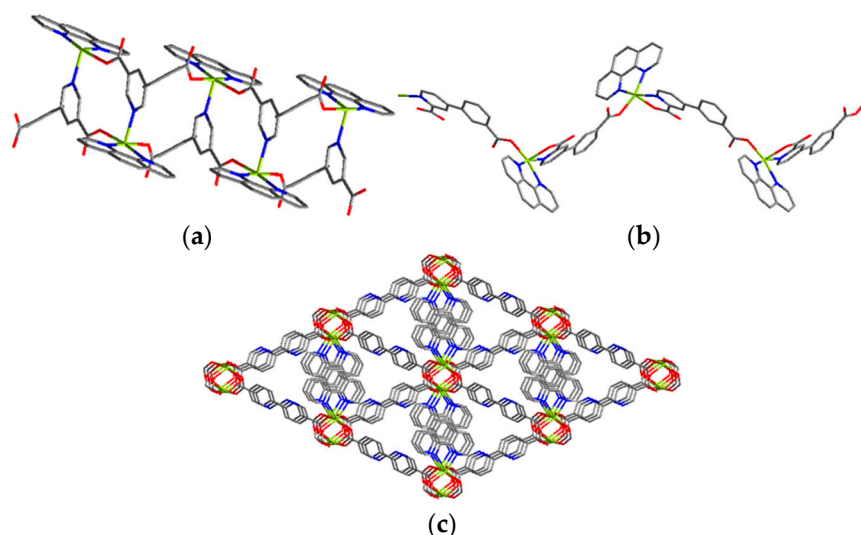


Figure 3. (a) 1D ladder chain in **1**. (b) 1D zigzag chain in **2**. (c) 3D metal-organic framework in **3**. Adapted from [42,44,45].

2.3. Effect of Metal Source

The type of metal node also plays an important structure-defining role in the hydrothermal generation of coordination polymers. This is primarily associated with different coordination behavior and ligand affinity of distinct metal centers, their charges and ionic radii. Selected examples of CPs

assembled under identical reaction conditions but using different metal sources are collected in Table 2. In particular, an interesting series of compounds **14**–**16** can be built from H₃btc and phen ligands by using different metal(II) chlorides, namely a 1D chain $\{[\text{Cd}(\mu_3\text{-Hbtc})(\text{phen})(\text{H}_2\text{O})]\cdot\text{H}_2\text{O}\}_n$ (**14**), a 3D MOF $[\text{Pb}_3(\mu_4\text{-Hbtc})_2(\text{phen})_2]_n$ (**15**), and a 0D monomer $[\text{Ni}(\text{Hbtc})_2(\text{phen})_2(\text{H}_2\text{O})]\cdot 2\text{H}_2\text{O}$ (**16**). Notably, despite the diversity of these structures, they all feature a monoprotonated tricarboxylic acid block, Hbtc²⁻.

Apart from the nature of metal, the type of anion in a starting metal salt can also influence the resulting structure. For example, samarium(III) coordination polymers $\{[\text{Sm}(\text{Hcpna})(\mu_4\text{-cpna})(\text{phen})_2]\cdot\text{H}_2\text{O}\}_n$ (3D net, **17**) and $\{[\text{Sm}(\text{Hcpna})(\mu_4\text{-cpna})(\text{phen})_2]\cdot 2\text{H}_2\text{O}\}_n$ (1D chain, **18**) were obtained under exactly the same conditions but using Sm(III) nitrate or chloride, respectively. MOF **17** reveals a very intricate structure, wherein the Sm₂ dimeric units are linked by the $\mu_4\text{-cpna}^{2-}$ ligands forming a dodecanuclear Sm₁₂ macrocycle (Figure 4a) that adopts a chair conformation. These Sm₁₂ units are then connected with six adjacent rings by corner-forming 2D layer motifs (Figure 4b), which are further linked by the coordination interaction with the cpna²⁻ blocks to furnish a very complex 3D framework (Figure 4c).

Table 2. Selected examples of CPs showing an effect of metal source on product structure.

Compound	Formula	Metal Source	Structure	Reference
10	$[\text{Co}(\mu\text{-cппa})(\text{phen})(\text{H}_2\text{O})]_n$	$\text{CoCl}_2\cdot 6\text{H}_2\text{O}$	1D zigzag chain	[44]
11	$\{[\text{Cd}_3(\mu_3\text{-cппa})_3(\text{phen})_2]\cdot 4\text{H}_2\text{O}\}_n$	$\text{CdCl}_2\cdot \text{H}_2\text{O}$	3D MOF	[44]
12	$\{[\text{Y}_2(\mu_4\text{-cpna})_3(\text{phen})_2(\text{H}_2\text{O})]\cdot \text{H}_2\text{O}\}_n$	$\text{Y}(\text{NO}_3)_3\cdot 6\text{H}_2\text{O}$	3D MOF	[43]
13	$[\text{Tm}(\mu_3\text{-cpna})(\text{phen})(\text{NO}_3)]_n$	$\text{Tm}(\text{NO}_3)_3\cdot 6\text{H}_2\text{O}$	1D double chain	[43]
14	$\{[\text{Cd}(\mu_3\text{-Hbtc})(\text{phen})(\text{H}_2\text{O})]\cdot \text{H}_2\text{O}\}_n$	$\text{CdCl}_2\cdot \text{H}_2\text{O}$	1D chain	[49]
15	$[\text{Pb}_3(\mu_4\text{-Hbtc})_2(\text{phen})]_n$	PbCl_2	3D MOF	[49]
16	$[\text{Ni}(\text{Hbtc})_2(\text{phen})_2(\text{H}_2\text{O})]\cdot 2\text{H}_2\text{O}$	$\text{NiCl}_2\cdot 6\text{H}_2\text{O}$	0D monomer	[50]
17	$\{[\text{Sm}(\text{Hcpna})(\mu_4\text{-cpna})(\text{phen})_2]\cdot \text{H}_2\text{O}\}_n$	$\text{Sm}(\text{NO}_3)_3\cdot 6\text{H}_2\text{O}$	3D MOF	[43]
18	$\{[\text{Sm}(\text{Hcpna})(\mu_4\text{-cpna})(\text{phen})_2]\cdot 2\text{H}_2\text{O}\}_n$	$\text{SmCl}_3\cdot 6\text{H}_2\text{O}$	1D chain	[43]

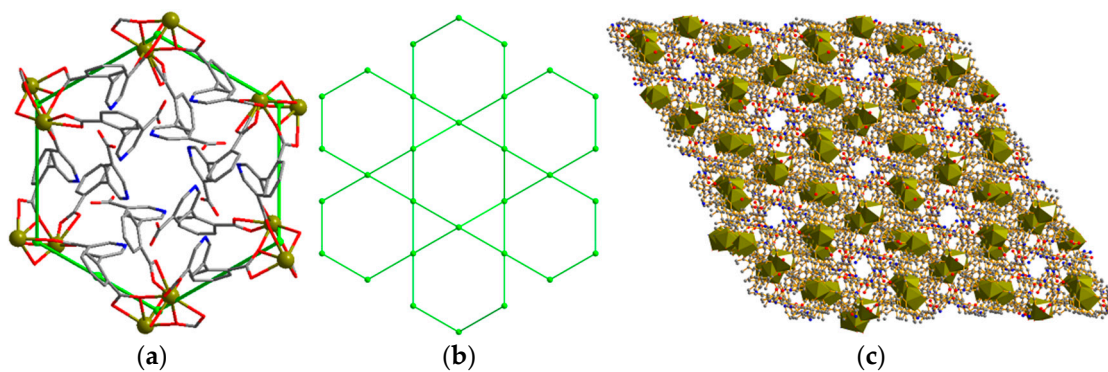


Figure 4. Structural fragments of MOF **17**. (a) Hexagonal Sm₁₂ macrocycle; green balls are Sm₂ units. (b) Interconnection of hexagonal macrocycles into a 2D layer motif; green balls are Sm₂ units. (c) 3D metal-organic framework. Adapted from [43].

2.4. Effect of Reagents Molar Ratio

In the synthesis of CPs, a proportion between metal node and main carboxylate ligand can be easily modified, what can cause a change of the coordination number of metal ions and affect the resulting structure. In addition, change of the molar ratio between main building block and alkali metal hydroxide used as a pH-regulator can result in a partial or full deprotonation of polycarboxylic acid ligand. As shown in Table 3, both 3D MOFs $\{[\text{Co}_3(\mu_4\text{-btc})_2(\mu\text{-H}_2\text{O})_2(\text{py})_4(\text{H}_2\text{O})_2]\cdot (\text{py})_2\}_n$ (**19**) and $\{[\text{Co}_{3.5}(\mu_6\text{-btc})_2(\mu_3\text{-OH})(\text{py})_2(\text{H}_2\text{O})_3]\cdot \text{H}_2\text{O}\}_n$ (**20**) were obtained under exactly the same conditions, except using a slightly different molar ratio between $\text{CoCl}_2\cdot 6\text{H}_2\text{O}$ and H₃btc (1.5:1 for **19** and 1.77:1 for **20**). However, these products feature very different structures and topologies (Figure 5). The structures

of product pairs **21/22** and **23/24** (Table 3) also differ significantly on varying the NaOH:H₂cppa and NaOH:H₃bptc molar ratios, respectively. In these cases, an excess of sodium hydroxide leads to a complete deprotonation of H₂cppa in **22** or a generation of additional μ_3 -OH linkers in **24**, thus making these structures more complicated in comparison with their counterparts assembled using a lower amount of NaOH.

Table 3. Selected examples of CPs showing an effect of reagents molar ratio on product structure.

Compound	Formula	Molar Ratio	Structure	Reference
19	$\{[\text{Co}_3(\mu_4\text{-btc})_2(\mu\text{-H}_2\text{O})_2(\text{py})_4(\text{H}_2\text{O})_2] \cdot (\text{py})_2\}_n$	CoCl ₂ :H ₃ btc = 1.5:1	3D MOF	[50]
20	$\{[\text{Co}_{3.5}(\mu_6\text{-btc})_2(\mu_3\text{-OH})(\text{py})_2(\text{H}_2\text{O})_3] \cdot \text{H}_2\text{O}\}_n$	CoCl ₂ :H ₃ btc = 1.77:1	3D MOF	[50]
21	$[\text{Ni}(\text{Hcppa})_2(\text{H}_2\text{O})_2] \cdot 2\text{H}_2\text{O}$	NaOH:H ₂ cppa = 1:1	0D monomer	[44]
22	$[\text{Ni}(\mu_3\text{-cppa})(\text{H}_2\text{O})_2]_n$	NaOH:H ₂ cppa = 2:1	2D layer	[44]
23	$\{[\text{Zn}_3(\mu_6\text{-bptc})_2(\text{H}_2\text{O})_4] \cdot \text{H}_2\text{O}\}_n$	NaOH:H ₃ bptc = 3:1	3D MOF	[51]
24	$[\text{Zn}_5(\mu_3\text{-OH})_4(\mu_6\text{-bptc})_2(\text{H}_2\text{O})_2]_n$	NaOH:H ₃ bptc = 5:1	3D MOF	[51]

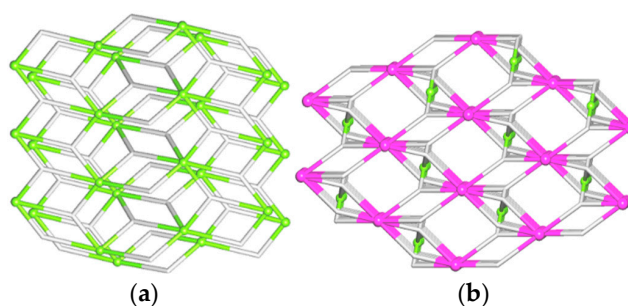


Figure 5. Topological representation of underlying 3D nets: (a) ant (anatase) net in **19**; (b) topologically unique net in **20** with the point symbol of $(4^2.6)_4(4^2.8^4)(4^6.6^4.8^{14}.10^4)$. Adapted from [50].

2.5. Effect of Reaction Temperature

The reaction temperature during the synthesis of metal-organic networks also has a significant impact on the final product structure. As illustrated in Table 4, compounds $\{[\text{Co}_2(\mu_3\text{-pyip})_2(\text{DMF})] \cdot (\text{solv})\}_n$ (**25**) and $\{[\text{Co}(\mu_3\text{-pyip})] \cdot 2\text{DMF}\}_n$ (**26**) were synthesized from exactly the same reaction mixtures but at different temperatures, 80 and 120 °C, respectively. These 3D MOFs feature distinct structures (Figure 6).

Table 4. Selected examples of CPs showing an effect of reaction temperature on product structure.

Compound	Formula	Temperature (°C)	Structure	Reference
25	$\{[\text{Co}_2(\mu_3\text{-pyip})_2(\text{DMF})] \cdot (\text{solv})\}_n$	80	3D MOF	[52]
26	$\{[\text{Co}(\mu_3\text{-pyip})] \cdot 2\text{DMF}\}_n$	120	3D MOF	[52]

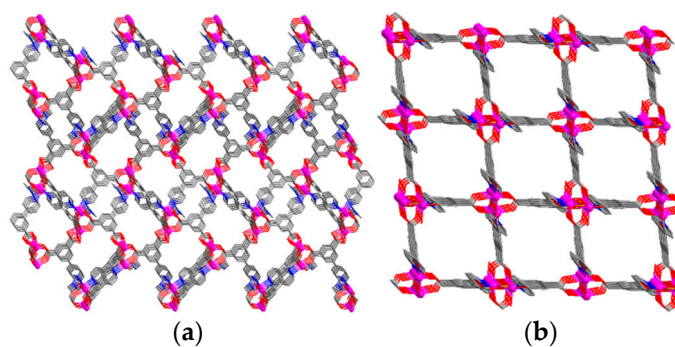


Figure 6. 3D metal-organic frameworks of **25** (a) and **26** (b). Adapted from [52].

2.6. Effect of Auxiliary Ligand

The presence of an additional auxiliary ligand also plays an important role in the hydrothermal synthesis of CPs, especially by facilitating product crystallization. Introduction of a common auxiliary *N,N*-donor ligand such as 2,2'-bipyridine or 1,10-phenanthroline usually changes the coordination environment of metal centers, thus resulting in the generation of different structures (Table 5). For example, the reaction of a cobalt(II) salt with H₂cppa with no auxiliary ligand leads to a 2D coordination polymer [Co(μ_3 -cppa)(H₂O)₂]_n (27), whereas simpler 1D zigzag chain products {[Co(μ -cppa)(2,2'-bpy)(H₂O)]·H₂O}_n (28) and [Co(μ -cppa)(phen)(H₂O)]_n (29) are generated in the presence of 2,2'-bpy or phen, respectively. Similarly, structurally distinct CPs {[Nd(μ -Hcpna)₂(μ -cpna)₂(H₂O)₂]·3H₂O}_n (34) and {[Nd(μ -Hcpna)₂(μ_4 -cpna)₂(phen)]·2H₂O}_n (35) (Figure 7) were prepared under the same synthetic conditions except the introduction of phen in 35. As can be seen from various examples collected in Table 5, the use of the *N,N*-donor auxiliary ligands tends to facilitate the formation of CPs with a lower dimensionality if compared to the systems without an auxiliary ligand. However, rather complex 3D MOF {[Cd₃(μ_5 -btc)₂(phen)₂(H₂O)]·H₂O}_n (31) can also be generated in the presence of the auxiliary ligand (Table 5).

Table 5. Selected examples of CPs showing an effect of auxiliary ligand on product structure.

Compound	Formula	Auxiliary Ligand	Structure	Reference
27	[Co(μ_3 -cppa)(H ₂ O) ₂] _n	no	2D network	[44]
28	[Co(μ -cppa)(2,2'-bpy)(H ₂ O)]·H ₂ O] _n	2,2'-bpy	1D zigzag chain	[44]
29	[Co(μ -cppa)(phen)(H ₂ O)] _n	phen	1D zigzag chain	[44]
30	[Cd ₃ (μ_6 -btc) ₂ (H ₂ O) ₅]·4H ₂ O] _n	no	3D MOF	[49]
31	[Cd ₃ (μ_5 -btc) ₂ (phen) ₂ (H ₂ O)]·H ₂ O] _n	phen	3D MOF	[49]
32	[Mn(μ_3 -cpna)(2,2'-bpy)(H ₂ O)] _n	2,2'-bpy	2D layer	[42]
33	[Mn(μ_3 -cpna)(phen)(H ₂ O)] _n	phen	1D ladder chain	[42]
34	[Nd(μ -Hcpna) ₂ (μ -cpna) ₂ (H ₂ O) ₂]·3H ₂ O] _n	no	2D layer	[42]
35	[Nd(μ -Hcpna) ₂ (μ_4 -cpna) ₂ (phen)]·2H ₂ O] _n	phen	1D double chain	[42]

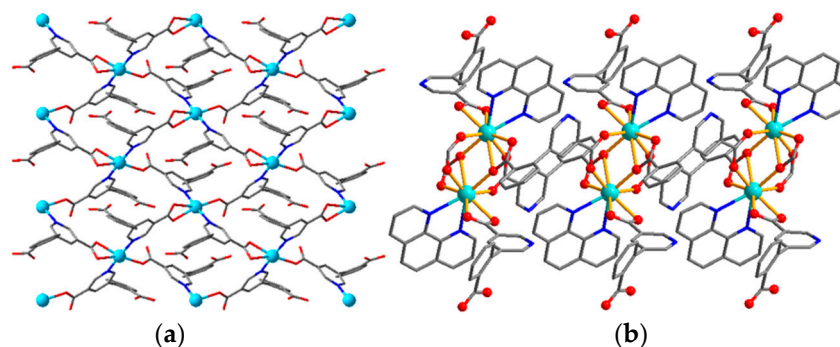


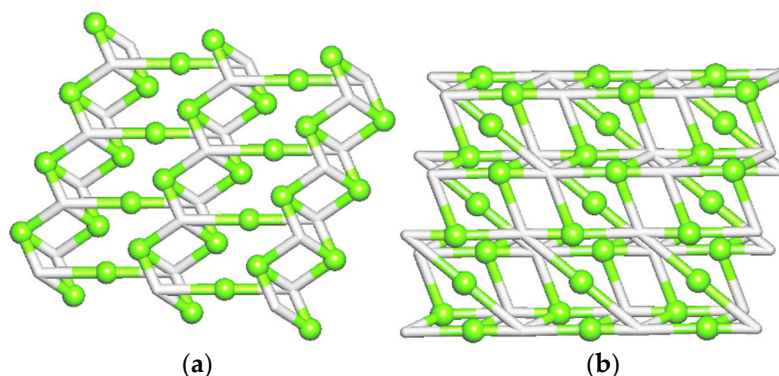
Figure 7. (a) 2D metal-organic layer in 34. (b) 1D double chain in 35. Adapted from [42].

2.7. Effect of Template

Template-assisted synthesis of CPs has attracted a special attention as a promising approach toward tunable architectures or structures that might be difficult to access by routine synthetic methods [47,53,54]. Various inorganic ions or organic molecules can be used as templating agents in the hydrothermal synthesis of coordination polymers. In particular, 4,4'-bipyridine acts not only as a common linker in CPs but is frequently applied as a template. Selected pairs of structurally distinct coordination polymers obtained with or without template are summarized in Table 6. For example, although compounds {[Ni₃(μ_4 -dcppa)₂(H₂O)₆]·2H₂O]_n (42) and {[Ni₃(μ_5 -dcppa)₂(H₂O)₆]·2H₂O]_n (43) were prepared under similar reaction conditions except using 4,4'-bipy as a templating agent in 43, they feature structures of different dimensionality and topology (Figure 8).

Table 6. Selected examples of CPs showing an effect of template on product structure.

Compound	Formula	Template	Structure	Reference
36	$[\text{Mn}_2(\mu_3\text{-pyip})_2(\text{H}_2\text{O})_4]\cdot 5\text{H}_2\text{O}]_n$	no	2D layer	[55]
37	$[\text{Mn}_3(\mu_5\text{-pyip})_2(\mu\text{-HCOO})_2(\text{H}_2\text{O})_2]_n$	4,4'-bpy	2D layer	[55]
38	$[\text{Co}(\mu_3\text{-pyip})(\text{EtOH})(\text{H}_2\text{O})]_n$	no	2D layer	[55]
39	$[\{\text{Co}(\mu_4\text{-pyip})(\text{H}_2\text{O})\}\cdot \text{H}_2\text{O}]_n$	cyanoacetic acid	2D double layer	[55]
40	$[\{\text{Mn}_3(\mu_4\text{-dcpa})_2(\text{H}_2\text{O})_6\}\cdot 3\text{H}_2\text{O}]_n$	no	2D layer	[47]
41	$[\{\text{Mn}_3(\mu_5\text{-dcpa})_2(\text{H}_2\text{O})_6\}\cdot 4\text{H}_2\text{O}]_n$	4,4'-bpy	3D MOF	[47]
42	$[\{\text{Ni}_3(\mu_4\text{-dcpa})_2(\text{H}_2\text{O})_6\}\cdot 2\text{H}_2\text{O}]_n$	no	2D layer	[47]
43	$[\{\text{Ni}_3(\mu_5\text{-dcpa})_2(\text{H}_2\text{O})_6\}\cdot 2\text{H}_2\text{O}]_n$	4,4'-bpy	3D MOF	[47]

**Figure 8.** Topological representation of underlying nets: (a) 2D layer with 3,4L83 topology in 42; (b) 3D framework with tcs topology in 43. Adapted from [47].

2.8. Effect of Two Main Ligands

Although a substantial number of coordination polymers incorporating various kinds of carboxylate ligands has been reported [56], the examples of heteroleptic networks constructed from a combination of two kinds of biphenyl or phenyl-pyridine carboxylate building blocks (Scheme 1) are barely known. It is primarily caused by different solubility of such ligands, distinct coordination modes and charges, as well as ligand competition for metal node during the hydrothermal synthesis and crystallization. The latter factor may often lead to the formation of a mixture of simpler products containing only one main building block rather than more complex products comprising both carboxylate ligands. The competition between two main carboxylate building blocks for metal nodes can be even more pronounced when the reaction mixture also contains an additional auxiliary ligand along with water as a solvent and frequent terminal ligand source. The effect of two different types of biphenyl carboxylate moieties on the structure of the resulting metal-organic network remains poorly studied. Notable examples of CPs combining two kinds of biphenyl carboxylate blocks include a 2D network $[\text{Cd}_2(\mu_5\text{-cpic})_2(\mu\text{-bpdc})_{0.5}(\text{phen})_2]_n$ (45) and a 3D MOF $[\text{Co}_2(\mu_7\text{-btc})_2(\mu\text{-bpydc})_{0.5}(\text{py})_3]_n$ (47) that feature distinct structures and topologies in comparison with their counterparts $[\{\text{Cd}_2(\mu_4\text{-cpic})(\mu_3\text{-OH})(\text{phen})_2\}\cdot 2\text{H}_2\text{O}]_n$ (44) and $[\{\text{Co}_3(\mu_4\text{-btc})_2(\mu\text{-H}_2\text{O})_2(\text{py})_4(\text{H}_2\text{O})_2\}\cdot (\text{py})_2]_n$ (46), respectively (Table 7, Figure 9).

Table 7. Selected examples of CPs showing an effect of two main carboxylate ligands on product structure.

Compound	Formula	Main Ligand	Structure	Reference
44	$[\{\text{Cd}_2(\mu_4\text{-cpic})(\mu_3\text{-OH})(\text{phen})_2\}\cdot 2\text{H}_2\text{O}]_n$	H ₃ cpic	2D layer	[57]
45	$[\text{Cd}_2(\mu_5\text{-cpic})_2(\mu\text{-bpdc})_{0.5}(\text{phen})_2]_n$	H ₃ cpic, H ₂ bpdc	2D layer	[57]
46	$[\{\text{Co}_3(\mu_4\text{-btc})_2(\mu\text{-H}_2\text{O})_2(\text{py})_4(\text{H}_2\text{O})_2\}\cdot (\text{py})_2]_n$	H ₃ btc	3D MOF	[50]
47	$[\text{Co}_2(\mu_7\text{-btc})_2(\mu\text{-bpydc})_{0.5}(\text{py})_3]_n$	H ₃ btc, H ₂ bpydc	3D MOF	[58]

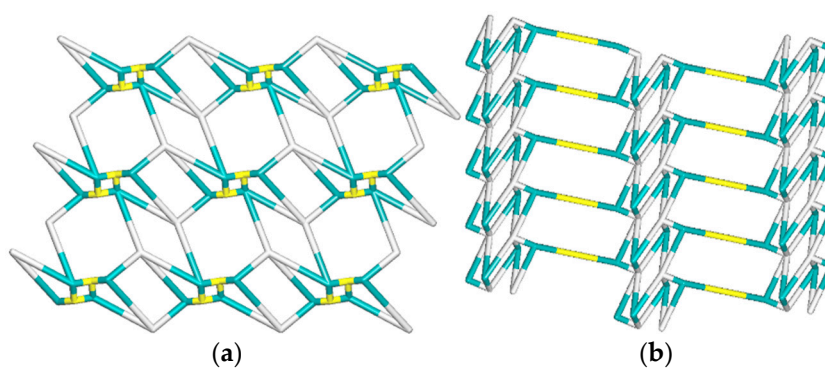


Figure 9. Topological representation of underlying nets: (a) 2D layer with 3,4L33 topology in 44; (b) trinodal 3,3,5-connected 2D layer in 45 with the unique topology and point symbol of $(4.6^2)(4^3)(4^4.6^4.8^2)$. Adapted from [57].

3. Selected Functional Properties and Applications

3.1. Highly Porous MOFs

Some coordination polymers based on multifunctional carboxylic acids with phenyl-pyridine or biphenyl cores possess the highly porous structures and excellent stability (Table 8). These properties make these materials rather promising for exploring CO₂ capture and gas storage applications. As illustrated in Table 8 and Figure 10, Zhao and co-workers synthesized a UiO type MOF derived from the H₂bpydc block, [Zr₆(μ₃-O)₄(OH)₄(μ-bpydc)₁₂] (50). This MOF exhibits high storage capacity for H₂, CH₄, and CO₂, showing an unusual stepwise adsorption for liquid CO₂ and solvents with a sequential filling mechanism on different adsorption sites. Other related MOFs with high porosity and interesting N₂, H₂, CO₂ and/or CH₄ uptake behavior include [Cu₂(μ₃-pyip)₂(H₂O)₂]_{0.5}[Cu(pyip)] (48), {[Cu(μ₃-pyip)]·2H₂O·1.5DMF}_n (49), and [Zn₃(μ₅-bpydc)₂(HCOO)₂]·H₂O·DMF (51) (Table 8).

Table 8. Selected examples of highly porous metal-organic frameworks (MOFs).

Compound	Formula	Porosity	Applications in Gas Uptake or Separation	Reference
48	[Cu ₂ (μ ₃ -pyip) ₂ (H ₂ O) ₂] _{0.5} [Cu(pyip)]	60.8%	N ₂ , H ₂ , CO ₂	[59]
49	{[Cu(μ ₃ -pyip)]·2H ₂ O·1.5DMF} _n	54.0%	N ₂ , H ₂ , CO ₂	[60]
50	[Zr ₆ (μ ₃ -O) ₄ (OH) ₄ (μ-bpydc) ₁₂]	68.5%	N ₂ , H ₂ , CO ₂ , CH ₄	[61]
51	[Zn ₃ (μ ₅ -bpydc) ₂ (HCOO) ₂]·H ₂ O·DMF	64.3%	N ₂ , CO ₂ , CH ₄	[62]

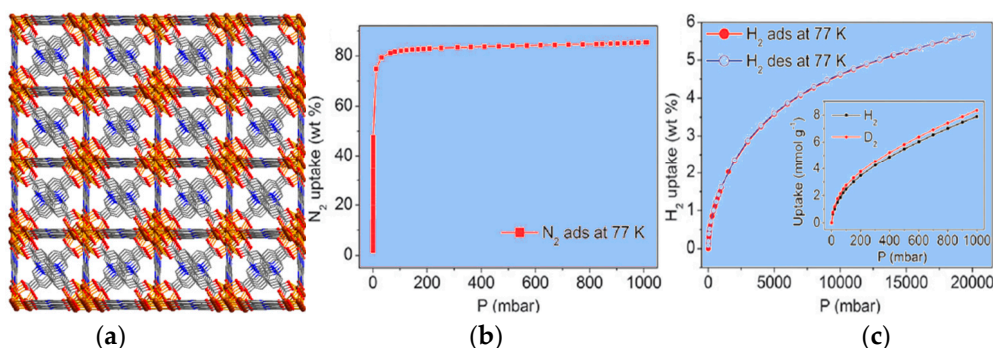


Figure 10. Cont.

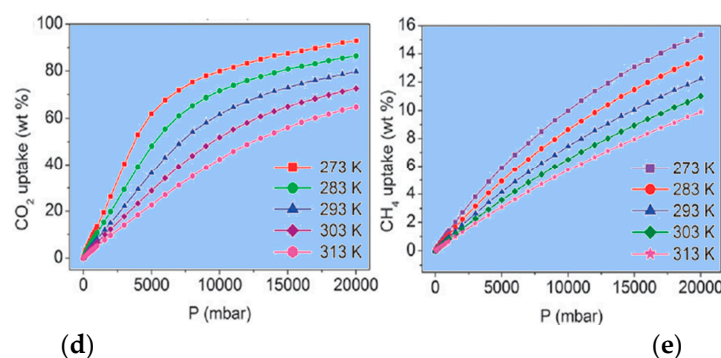


Figure 10. (a) 3D metal-organic framework of **50**. (b–e) Adsorption isotherms of **50** for (b) N_2 , (c) H_2 and D_2 (inset), (d) CO_2 , and (e) CH_4 . Adapted from [61].

3.2. Highly Luminescent Materials

MOFs based on the europium(III) and terbium(III) nodes are highly luminescent compounds. As illustrated in Table 9 and Figure 11, an interesting example concerns a Tb MOF $[Tb(\mu_4\text{-bpydc})(\mu_3\text{-HCOO})]_n$ (**53**) derived from the $H_2\text{bpydc}$ building block. It features a remarkable temperature-dependent photoluminescence. At 298 K, under UV excitation, compound **53** glows red-orange, whereas at 77 K it emits a green light. Another example concerns a Eu(III) derivative $[Eu_2(\mu_4\text{-pyip})_3(H_2O)_4]_n \cdot 2n\text{DMF} \cdot 3nH_2O$ (**52**) that is capable of emitting different colors ranging from yellow to red and orange.

Table 9. Selected examples of highly luminescent MOFs.

Compound	Formula	λ_{em} (nm)	Color	Reference
52	$[Eu_2(\mu_4\text{-pyip})_3(H_2O)_4]_n \cdot 2n\text{DMF} \cdot 3nH_2O$	255–365	yellow to red and then to orange	[63]
53	$[Tb(\mu_4\text{-bpydc})(\mu_3\text{-HCOO})]_n$	614, 541	red-orange (298 K), green (77 K)	[64]

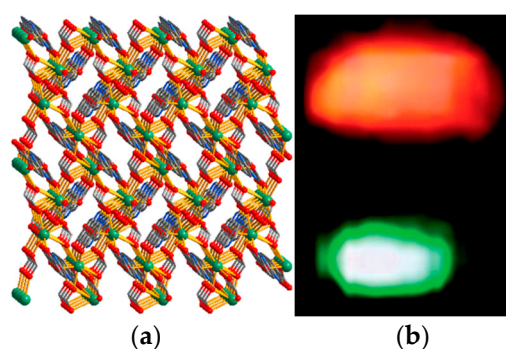


Figure 11. (a) 3D metal-organic framework of **53**; (b) temperature-dependent red-orange (top, 298 K) or green (bottom, 77 K) emission under UV excitation. Adapted from [64].

3.3. Compounds with Unusual Magnetic Properties

Some coordination polymers derived from multifunctional carboxylic acids with phenyl-pyridine or biphenyl cores can exhibit unusual magnetic properties. Selected examples are highlighted in Table 10. In particular, Du and co-workers assembled a 3D MOF, $[[Dy_2(\mu_4\text{-pyip})_3(H_2O)_4] \cdot 2\text{DMF} \cdot 3H_2O]_n$ (**54**), using $H_2\text{pyip}$ as a building block. This compound possesses the **pcu** topology and exhibits a slow magnetization relaxation behavior (Figure 12). Other notable examples of magnetic CPs include a nickel(II) derivative $[Ni_3(\mu_5\text{-pyip})_2(\mu\text{-HCOO})_2(H_2O)_2]_n$ (**55**) with a long-range magnetic ordering as well as the dysprosium(III)

$[\text{Dy}(\mu_5\text{-bptc})(\text{phen})(\text{H}_2\text{O})]_n$ (**56**) and $\{[\text{Dy}_3\text{Co}_2(\mu_4\text{-bpydc})_5(\mu_3\text{-Hbpydc})(\text{H}_2\text{O})_5](\text{ClO}_4)_2\}_n$ (**57**) frameworks with a slow magnetization relaxation behavior.

Table 10. Selected examples of CPs with unusual magnetic properties.

Compound	Formula	Magnetic Behavior	Highlight	Reference
54	$\{[\text{Dy}_2(\mu_4\text{-pyip})_3(\text{H}_2\text{O})_4]\cdot 2\text{DMF}\cdot 3\text{H}_2\text{O}\}_n$	weak ferromagnetic	slow magnetization relaxation behavior	[63]
55	$[\text{Ni}_3(\mu_5\text{-pyip})_2(\mu\text{-HCOO})_2(\text{H}_2\text{O})_2]_n$	weak ferromagnetic	long-range magnetic ordering	[65]
56	$[\text{Dy}(\mu_5\text{-bptc})(\text{phen})(\text{H}_2\text{O})]_n$	antiferromagnetic	slow magnetization relaxation behavior	[66]
57	$\{[\text{Dy}_3\text{Co}_2(\mu_4\text{-bpydc})_5(\mu_3\text{-Hbpydc})(\text{H}_2\text{O})_5](\text{ClO}_4)_2\cdot 11\text{H}_2\text{O}\}_n$	antiferromagnetic	slow magnetization relaxation behavior	[67]

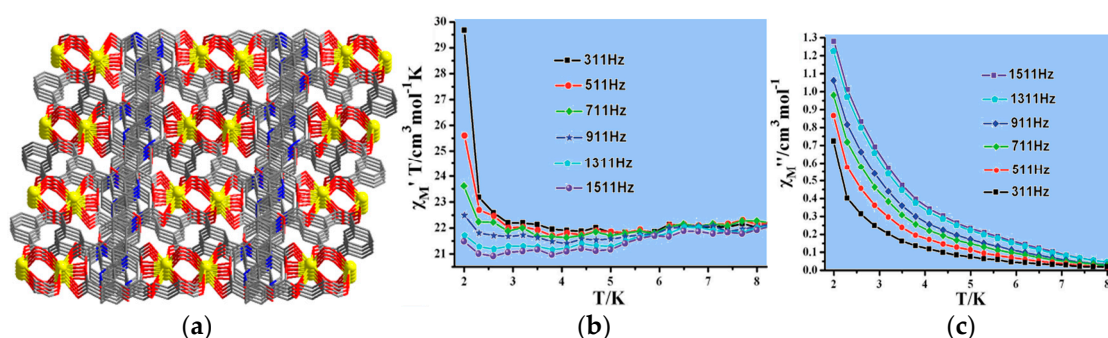


Figure 12. (a) 3D metal-organic framework of **54**. (b,c) Ac susceptibility of **54** measured in zero dc fields and plotted as $\chi'T$ vs. T (b) and χ'' vs. T (c). Adapted from [63].

3.4. Selective Sensing Materials

It is known that some fluorescent MOF materials are sensitive to the presence or absence of guest solvent molecules. As illustrated in Table 11 and Figure 13, Wen and co-workers reported a 3D MOF based on the H_2pyip ligand, $[\text{Zn}(\mu_3\text{-pyip})(\text{bimb})\cdot(\text{H}_2\text{O})]_n$ (**58**). This MOF exhibits the first report of a MOF material as a promising luminescent probe for detecting pesticides. This compound is also unique by allowing a detection of both pesticides and solvent molecules simultaneously. Other examples of sensing MOFs are shown in Table 11.

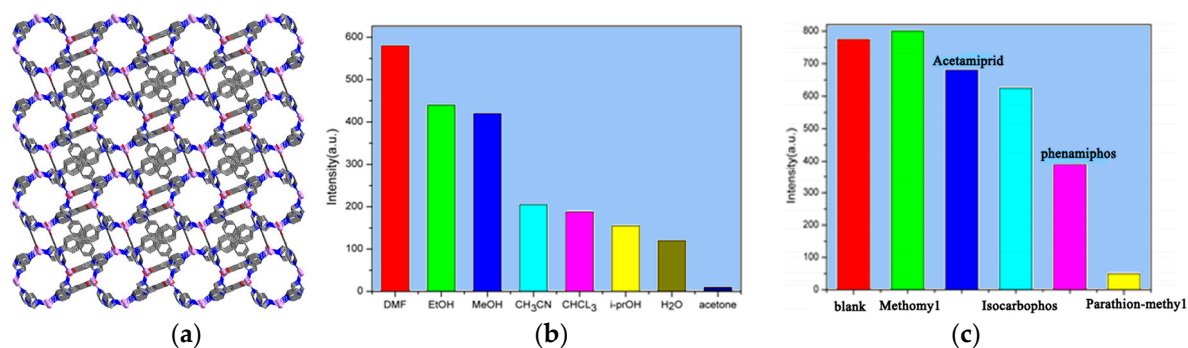


Figure 13. (a) 3D metal-organic framework of **58**. (b,c) Photoluminescence intensities of **58** introduced to (b) various pure solvents or (c) different pesticides (1×10^{-3} M in DMF); $\lambda_{\text{ex}} = 290$ nm. Adapted from [68].

Table 11. Selected examples of MOFs with selective sensing behavior.

Compound	Formula	Structure	Analyte	Reference
58	$[\text{Zn}(\mu_3\text{-pyip})(\text{bimb})\cdot(\text{H}_2\text{O})]_n$	3D MOF	acetone, pesticides	[68]
59	$[\text{Zr}_6(\mu_3\text{-O})_4(\text{OH})_4(\mu_4\text{-bpydc})_{12}]_n$	3D MOF	Fe^{3+} ions	[69]
60	$[\text{Eu}_2(\mu_4\text{-bpydc})_3(\text{H}_2\text{O})_3]_n \cdot n\text{DMF}$	3D MOF	Cu^{2+} ions	[69]

4. Conclusions and Outlook

In this mini-review, we featured selected recent examples of coordination polymers (CPs) or metal-organic frameworks (MOFs) that were constructed from various multifunctional carboxylic acids with phenyl-pyridine or biphenyl cores (Scheme 1). Despite being still little explored, these types of semi-rigid, thermally stable, and versatile building blocks appear to be very promising for the hydrothermal synthesis of metal-organic networks with different structural characteristics, topologies, and functional properties. The present work also highlighted an importance of different reaction parameters and conditions on the assembly and structural diversity of coordination polymers. The effects of the type of main carboxylate ligand, kind of metal node, stoichiometry and molar ratio of reagents, temperature, presence or absence of auxiliary ligands or templates were showcased. In addition, some examples of highly porous MOFs, notable luminescent materials, compounds with unusual magnetic properties, and frameworks for selective sensing applications were described.

We believe the application of multifunctional carboxylic acids containing phenyl-pyridine or biphenyl cores toward the design of coordination polymers will be continued, leading to new series of coordination compounds and derived materials with fascinating structural features and notable functional properties. Future research might focus on: (A) widening the family of multicarboxylate building blocks to new members with additional functional groups; (B) diversifying the types of metal nodes; (C) assembling heterometallic metal-organic architectures; (D) optimizing the conditions of the hydrothermal synthesis and crystallization; (E) predicting the structural and topological characteristics; and (F) broadening the types of possible applications of the obtained coordination polymers.

Acknowledgments: This work was financially supported by the National Natural Science Foundation of China (Project 21572086). AMK and MVK acknowledge the Foundation for Science and Technology (FCT), Portugal (UID/QUI/00100/2013, IF/01395/2013/CP1163/CT005).

Conflicts of Interest: The authors declare no conflict of interest.

Abbreviations

0D	zero-dimensional
1D	one-dimensional
2D	two-dimensional
3D	three-dimensional
CP	coordination polymer
MOF	metal-organic framework
H_2cpna	5-(2'-carboxylphenyl)-nicotinic acid
H_2pyip	5-(4-pyridyl)-isophthalic acid
H_2cppa	4-(3-carboxyphenyl)-picolinic acid
H_2bpydc	2,2'-bipyridine-5,5'-dicarboxylic acid
H_3bptc	biphenyl-2,5,3'-tricarboxylic acid
H_3btc	biphenyl-2,4,4'-tricarboxylic acid
H_3cpic	4-(5-carboxypyridin-2-yl)-isophthalic acid
H_3cptc	2-(4-carboxypyridin-3-yl)-terephthalic acid
H_3dcppa	5-(6-carboxypyridin-3-yl)-isophthalic acid
H_3cpta	2-(5-carboxypyridin-2-yl)-terephthalic acid
py	pyridine
phen	1,10-phenanthroline

2,2'-bpy	2,2'-bipyridine
4,4'-bpy	4,4'-bipyridine
H ₂ biim	2,2'-biimidazole
H ₂ bpdc	4,4'-biphenyldicarboxylic acid
bimb	4,4'-bis(1-imidazolyl)biphenyl

References

- Batten, S.R.; Champness, N.R.; Chen, X.M.; Garcia-Martinez, J.; Kitagawa, S.; Öhrström, L.; O’Keeffe, M.; Suh, M.P.; Reedijk, J. Terminology of metal-organic frameworks and coordination polymers (IUPAC Recommendations 2013). *Pure Appl. Chem.* **2013**, *85*, 1715–1724. [[CrossRef](#)]
- Kaskel, S. (Ed.) *The Chemistry of Metal-Organic Frameworks: Synthesis, Characterization, and Applications*; Wiley: Hoboken, NJ, USA, 2016; p. 904.
- Banerjee, R. (Ed.) *Functional Supramolecular Materials: From Surfaces to MOFs*; RSC: London, UK, 2017; p. 461.
- MacGillivray, L.R.; Lukehart, C.M. (Eds.) *Metal-Organic Framework Materials*; Wiley: Hoboken, NJ, USA, 2014; p. 592.
- Farrusseng, D. (Ed.) *Metal-Organic Frameworks: Applications from Catalysis to Gas Storage*; Wiley: Hoboken, NJ, USA, 2011; p. 414.
- Batten, S.R.; Neville, S.M.; Turner, D.R. *Coordination Polymers: Design, Analysis and Application*; RSC: London, UK, 2009; p. 424.
- Schmidt, F.M.S.; Merkel, M.P.; Kostakis, G.E.; Buth, G.; Anson, C.E.; Powell, A.K. SMM behaviour and magnetocaloric effect in heterometallic 3d-4f coordination clusters with high azide: Metal ratios. *Dalton Trans.* **2017**, *46*, 15661–15665. [[CrossRef](#)] [[PubMed](#)]
- Kallitsakis, M.; Loukopoulos, E.; Abdul-Sada, A.; Tizzard, G.J.; Coles, S.J.; Kostakis, G.E.; Lykakis, I.N. A copper-benzotriazole-based coordination polymer catalyzes the efficient one-pot synthesis of (N''-substituted)-hydrazo-4-aryl-1,4-dihydropyridines from Azines. *Adv. Synth. Catal.* **2017**, *359*, 138–145. [[CrossRef](#)]
- Catala, L.; Mallah, T. Nanoparticles of prussian blue analogs and related coordination polymers: From information storage to biomedical applications. *Coord. Chem. Rev.* **2017**, *346*, 32–61. [[CrossRef](#)]
- Islamoglu, T.; Goswami, S.; Li, Z.Y.; Howarth, A.J.; Farha, O.K.; Hupp, J.T. Postsynthetic tuning of metal-organic frameworks for targeted applications. *Acc. Chem. Res.* **2017**, *50*, 805–813. [[CrossRef](#)] [[PubMed](#)]
- Lusby, P.J. Supramolecular coordination chemistry. *Annu. Rep. Prog. Chem. Sect. A* **2010**, *106*, 319–339. [[CrossRef](#)]
- Liu, S.J.; Chen, Y.; Xu, W.J.; Zhao, Q.; Huang, W. New trends in the optical and electronic applications of polymers containing transition-metal complexes. *Macromol. Rapid Commun.* **2012**, *33*, 461–480. [[CrossRef](#)] [[PubMed](#)]
- Kaur, R.; Kim, K.H.; Paul, A.K.; Akash, D. Recent advances in the photovoltaic applications of coordination polymers and metal organic frameworks. *J. Mater. Chem. A* **2016**, *4*, 3991–4002. [[CrossRef](#)]
- He, C.B.; Liu, D.M.; Lin, W.B. Nanomedicine applications of hybrid nanomaterials built from metal-ligand coordination bonds: Nanoscale metal-organic frameworks and nanoscale coordination polymers. *Chem. Rev.* **2015**, *115*, 11079–11108. [[CrossRef](#)] [[PubMed](#)]
- Mai, H.D.; Rafiq, K.; Yoo, H. Nano metal-organic framework-derived inorganic hybrid nanomaterials: Synthetic strategies and applications. *Chem. Eur. J.* **2017**, *23*, 5631–5651. [[CrossRef](#)] [[PubMed](#)]
- Cui, Y.J.; Li, B.; He, H.J.; Zhou, W.; Chen, B.L.; Qian, G.D. Metal-organic frameworks as platforms for functional materials. *Acc. Chem. Res.* **2016**, *49*, 483–493. [[CrossRef](#)] [[PubMed](#)]
- Dolgoplova, E.A.; Brandt, A.J.; Ejegbavwo, O.A.; Duke, A.S.; Maddumapatabandi, T.D.; Galhenage, R.P.; Larson, B.W.; Reid, O.G.; Ammal, S.C.; Heyden, A.; et al. Electronic properties of bimetallic metal-organic frameworks (MOFs): Tailoring the density of electronic states through MOF modularity. *J. Am. Chem. Soc.* **2017**, *139*, 5201–5209. [[CrossRef](#)] [[PubMed](#)]
- Kirillov, A.M.; Wiczorek, S.W.; Lis, A.; da Silva, M.F.C.G.; Florek, M.; Król, J.; Staroniewicz, Z.; Smolenski, P.; Pombeiro, A.J.L. 1,3,5-Triaza-7-phosphaadamantane-7-oxide (PTA=O): New diamondoid building block for design of 3D metal-organic frameworks. *Cryst. Growth Des.* **2011**, *11*, 2711–2716. [[CrossRef](#)]

19. Dias, S.S.P.; Kirillova, M.V.; André, V.; Kłak, J.; Kirillov, A.M. New tetracopper(II) cubane cores driven by a diamino alcohol: Self-assembly synthesis, structural and topological features, and magnetic and catalytic oxidation properties. *Inorg. Chem.* **2015**, *54*, 5204–5212. [[CrossRef](#)] [[PubMed](#)]
20. Lemaire, P.C.; Lee, D.T.; Zhao, J.J.; Parsons, G.N. Reversible low-temperature metal node distortion during atomic layer deposition of Al₂O₃ and TiO₂ on UiO-66-NH₂ metal organic framework crystal surfaces. *ACS Appl. Mater. Interfaces* **2017**, *9*, 22042–22054. [[CrossRef](#)] [[PubMed](#)]
21. Ji, P.F.; Manna, K.; Lin, Z.; Urban, A.; Greene, F.X.; Lan, G.X.; Lin, W.B. Single-site cobalt catalysts at new Zr₈(μ₂-O)₈(μ₂-OH)₄ metal-organic framework nodes for highly active hydrogenation of alkenes, imines, carbonyls, and heterocycles. *J. Am. Chem. Soc.* **2016**, *138*, 12234–12242. [[CrossRef](#)] [[PubMed](#)]
22. Jaros, S.W.; Silva, M.F.C.G.D.; Florek, M.; Oliveira, M.C.; Smoleński, P.; Pombeiro, A.J.L.; Kirillov, A.M. Aliphatic dicarboxylate directed assembly of silver(I) 1,3,5-Triaza-7-phosphaadamantane coordination networks: Topological versatility and antimicrobial activity. *Cryst. Growth Des.* **2014**, *14*, 5408–5417. [[CrossRef](#)]
23. Wang, K.B.; Geng, Z.R.; Zheng, M.B.; Ma, L.Y.; Ma, X.Y.; Wang, Z.L. Controllable fabrication of coordination polymer particles (CPPs): A bridge between versatile organic building blocks and porous copper-based inorganic materials. *Cryst. Growth Des.* **2012**, *12*, 5606–5614. [[CrossRef](#)]
24. Manna, P.; Das, S.K. Perceptive approach in assessing rigidity versus flexibility in the construction of diverse metal-organic coordination networks: Synthesis, structure, and magnetism. *Cryst. Growth Des.* **2015**, *15*, 1407–1421. [[CrossRef](#)]
25. Beeching, L.J.; Hawes, C.S.; Turnera, D.R.; Batten, S.R. The influence of anion, ligand geometry and stoichiometry on the structure and dimensionality of a series of AgI-bis(cyanobenzyl)piperazine coordination polymers. *CrystEngComm* **2014**, *16*, 6459–6468. [[CrossRef](#)]
26. Xu, W.; Si, Z.X.; Xie, M.; Zhou, L.X.; Zheng, Y.Q. Experimental and theoretical approaches to three uranyl coordination polymers constructed by phthalic acid and N,N'-donor bridging ligands: crystal structures, luminescence, and photocatalytic degradation of tetracycline hydrochloride. *Cryst. Growth Des.* **2017**, *17*, 2147–2157. [[CrossRef](#)]
27. Kobayashi, Y.; Honjo, K.; Kitagawa, S.; Uemura, T. Preparation of porous polysaccharides templated by coordination polymer with three-dimensional nanochannels. *ACS Appl. Mater. Interfaces* **2017**, *9*, 11373–11379. [[CrossRef](#)] [[PubMed](#)]
28. Ding, R.; Huang, C.; Lu, J.J.; Wang, J.N.; Song, C.J.; Wu, J.; Hou, H.W.; Fan, Y.T. Solvent templates induced porous metal-organic materials: Conformational isomerism and catalytic activity. *Inorg. Chem.* **2015**, *54*, 1405–1413. [[CrossRef](#)] [[PubMed](#)]
29. Garai, M.; Maji, K.; Chernyshev, V.V.; Biradha, K. Interplay of pyridine substitution and Ag(I)⋯Ag(I) and Ag(I)⋯π interactions in templating photochemical solid state [2+2] reactions of unsymmetrical olefins containing amides: Single-crystal-to-single-crystal transformations of coordination polymers. *Cryst. Growth Des.* **2016**, *16*, 550–554. [[CrossRef](#)]
30. Wang, J.; Bai, C.; Hua, H.M.; Yuan, F.; Xue, G.L. A family of entangled coordination polymers constructed from a flexible V-shaped long bicarboxylic acid and auxiliary N-donor ligands: Luminescent sensing. *J. Solid State Chem.* **2017**, *249*, 87–97. [[CrossRef](#)]
31. Zhang, J.Y.; Shi, J.X.; Chen, L.Y.; Jia, Q.X.; Deng, W.; Gao, E.Q. N-donor auxiliary ligand-directed assembly of Co^{II} compounds with a 2,2'-dinitro-biphenyl-4,4'-dicarboxylate ligand: Structures and magnetic properties. *CrystEngComm* **2017**, *19*, 1738–1750. [[CrossRef](#)]
32. Ren, Y.L.; Li, L.; Mu, B.; Li, C.X.; Huang, R.D. Electrocatalytic properties of three new POMs-based inorganic-organic frameworks with flexible zwitterionic dicarboxylate ligands. *J. Solid State Chem.* **2017**, *249*, 1–8. [[CrossRef](#)]
33. Hu, K.Q.; Zhu, L.Z.; Wang, C.Z.; Mei, L.; Liu, Y.H.; Gao, Z.Q.; Chai, Z.F.; Shi, W.Q. Novel uranyl coordination polymers based on quinoline-containing dicarboxylate by altering auxiliary ligands: From 1D chain to 3D framework. *Cryst. Growth Des.* **2016**, *16*, 4886–4896. [[CrossRef](#)]
34. Yang, L.Z.; Wang, J.; Kirillov, A.M.; Dou, W.; Xu, C.; Fang, R.; Xu, C.L.; Liu, W.S. 2D lanthanide MOFs driven by a rigid 3,5-bis(3-carboxy-phenyl)pyridine building block: Solvothermal syntheses, structural features, and photoluminescence and sensing properties. *CrystEngComm* **2016**, *18*, 6425–6436. [[CrossRef](#)]
35. Song, J.F.; Jia, Y.Y.; Zhou, R.S.; Li, S.Z.; Qiu, X.M.; Liu, J. Six new coordination compounds based on rigid 5-(3-carboxy-phenyl)-pyridine-2-carboxylic acid: Synthesis, structural variations and properties. *RSC Adv.* **2017**, *7*, 7217–7226. [[CrossRef](#)]

36. Øien, S.; Agostini, G.; Svelle, S.; Borfecchia, E.; Lomachenko, K.A.; Mino, L.; Gallo, E.; Bordiga, S.; Olsbye, U.; Lillerud, K.P.; et al. Probing reactive platinum sites in UiO-67 zirconium metal-organic frameworks. *Chem. Mater.* **2015**, *27*, 1042–1056.
37. Amarante, T.R.; Neves, P.; Valente, A.A.; Paz, F.A.A.; Fitch, A.N.; Pillinger, M.; Gonçalves, I.S. Hydrothermal synthesis, crystal structure, and catalytic potential of a one-dimensional molybdenum oxide/bipyridinedicarboxylate hybrid. *Inorg. Chem.* **2013**, *52*, 4618–4628. [[CrossRef](#)] [[PubMed](#)]
38. Maza, W.A.; Padilla, R.; Morris, A.J. Concentration dependent dimensionality of resonance energy transfer in a postsynthetically doped morphologically homologous analogue of UiO-67 MOF with a ruthenium(II) polypyridyl complex. *J. Am. Chem. Soc.* **2015**, *137*, 8161–8168. [[CrossRef](#)] [[PubMed](#)]
39. Robin, A.Y.; Fromm, K.M. Coordination polymer networks with O- and N-donors: What they are, why and how they are made. *Coord. Chem. Rev.* **2006**, *250*, 2127–2157. [[CrossRef](#)]
40. Byrappa, K.; Yoshimura, M. *Handbook of Hydrothermal Technology: A Technology for Crystal Growth and Materials Processing*; William Andrew Publishing, LLC Norwich: New York, NY, USA, 2001.
41. Kitagawa, S.; Noro, S. Coordination polymers: Infinite systems. *Compr. Coord. Chem.* **2003**, *7*, 231–256.
42. Gu, J.Z.; Gao, Z.Q.; Tang, Y. pH and auxiliary ligand influence on the structural variations of 5-(2'-Carboxylphenyl) nicotinate coordination polymers. *Cryst. Growth Des.* **2012**, *12*, 3312–3323. [[CrossRef](#)]
43. Gu, J.Z.; Wu, J.; Lv, D.Y.; Tang, Y.; Zhu, K.Y.; Wu, J.C. Lanthanide coordination polymers based on 5-(2'-carboxylphenyl) nicotinate: Syntheses, structure diversity, dehydration/hydration, luminescence and magnetic properties. *Dalton Trans.* **2013**, *42*, 4822–4830. [[CrossRef](#)] [[PubMed](#)]
44. Gu, J.Z.; Liang, X.X.; Cui, Y.H.; Wu, J.; Kirillov, A.M. Exploring 4-(3-carboxyphenyl)picolinic acid as a semirigid building block for the hydrothermal self-assembly of diverse metal-organic and supramolecular networks. *CrystEngComm* **2017**, *19*, 117–118. [[CrossRef](#)]
45. Zhang, G.M.; Li, Y.; Zou, X.Z.; Zhang, J.A.; Gu, J.Z.; Kirillov, A.M. Nickel(II) and manganese(II) metal-organic networks driven by 2,2'-bipyridine-5,5'-dicarboxylate blocks: synthesis, structural features, and magnetic properties. *Transit. Met. Chem.* **2016**, *41*, 153–160. [[CrossRef](#)]
46. Shao, Y.L.; Cui, Y.H.; Gu, J.Z.; Kirillov, A.M.; Wu, J.; Wang, Y.W. A variety of metal-organic and supramolecular networks constructed from a new flexible multifunctional building block bearing picolinate and terephthalate functionalities: hydrothermal self-assembly, structural features, magnetic and luminescent properties. *RSC Adv.* **2015**, *5*, 87484–87495. [[CrossRef](#)]
47. Gu, J.Z.; Cui, Y.H.; Liang, X.X.; Wu, J.; Lv, D.Y.; Kirillov, A.M. Structurally distinct metal-organic and H-Bonded networks derived from 5-(6-Carboxypyridin-3-yl)isophthalic acid: Coordination and template effect of 4,4'-bipyridine. *Cryst. Growth Des.* **2016**, *16*, 4658–4670. [[CrossRef](#)]
48. Li, Y.; Zhou, Q.; Gu, J.Z.; You, A. Syntheses, crystal structures, and magnetic properties of Mn(II) and Co(II) coordination polymers constructed from pyridine-tricarboxylate ligand. *Chin. J. Struct. Chem.* **2017**, *36*, 661–670.
49. Gu, J.Z.; Kirillov, A.M.; Wu, J.; Lv, D.Y.; Tang, Y.; Wu, J.C. Synthesis, structural versatility, luminescent and magnetic properties of a series of coordination polymers constructed from biphenyl-2,4,4'-tricarboxylate and different N-donor ligands. *CrystEngComm* **2013**, *15*, 10287–10303. [[CrossRef](#)]
50. Shao, Y.L.; Cui, Y.H.; Gu, J.Z.; Wu, J.; Wang, Y.W.; Kirillov, A.M. Exploring biphenyl-2,4,4'-tricarboxylic acid as a flexible building block for the hydrothermal self-assembly of diverse metal-organic and supramolecular networks. *CrystEngComm* **2016**, *18*, 765–778. [[CrossRef](#)]
51. Wu, W.P.; Liu, B.; Yang, G.P.; Miao, H.H.; Xi, Z.P.; Wang, Y.Y. Two new pH-controlled coordination polymers constructed from an asymmetrical tricarboxylate ligand and Zn-based rod-shaped SBUs. *Inorg. Chem. Commun.* **2015**, *56*, 8–12. [[CrossRef](#)]
52. Jia, G.H.; Athwal, H.S.; Blake, A.J.; Champness, N.R.; Hubberstey, P.; Schroder, M. Increasing nuclearity of secondary building units in porous cobalt(II) metal-organic frameworks: Variation in structure and H₂ adsorption. *Dalton Trans.* **2011**, *40*, 12342–12349. [[CrossRef](#)] [[PubMed](#)]
53. Stock, N.; Biswas, S. Synthesis of metal-organic frameworks (MOFs): Routes to various MOF topologies, morphologies, and composites. *Chem. Rev.* **2012**, *112*, 933–969. [[CrossRef](#)] [[PubMed](#)]
54. Lu, Y.B.; Jian, F.M.; Jin, S.; Zhao, J.W.; Xie, Y.R.; Luo, G.T. Three-dimensional extended frameworks constructed from dinuclear lanthanide(III) 1,4-naphthalenedicarboxylate units with bis(2,2'-biimidazole) templates: Syntheses, structures, and magnetic and luminescent properties. *Cryst. Growth Des.* **2014**, *14*, 1684–1694. [[CrossRef](#)]

55. Liu, Y.Y.; Li, H.J.; Han, Y.; Lv, X.F.; Hou, H.W.; Fan, Y.T. Template-assisted synthesis of Co, Mn-MOFs with magnetic properties based on pyridinedicarboxylic acid. *Cryst. Growth Des.* **2012**, *12*, 3505–3513. [[CrossRef](#)]
56. Groom, C.R.; Bruno, I.J.; Lightfoot, M.P.; Ward, S.C. Cambridge Structural Database. *Acta Cryst.* **2016**, *B72*, 171–179.
57. Gu, J.Z.; Cui, Y.H.; Wu, J.; Kirillov, A.M. A series of mixed-ligand 2D and 3D coordination polymers assembled from a novel multifunctional pyridine-tricarboxylate building block: Hydrothermal syntheses, structural and topological diversity, and magnetic and luminescent properties. *RSC Adv.* **2015**, *5*, 78889–78901. [[CrossRef](#)]
58. Li, W.B.; Gao, Z.Q.; Gu, J.Z. Synthesis, crystal structure, and magnetic properties of a Co metal-organic framework with mixed dicarboxylate and tricarboxylate ligands. *Chin. J. Struct. Chem.* **2016**, *35*, 257–263.
59. Lin, Q.P.; Bu, X.H.; Feng, P.Y. Perfect statistical symmetrization of a heterofunctional ligand induced by pseudo-copper trimer in an expanded matrix of HKUST-1. *Cryst. Growth Des.* **2013**, *13*, 5175–5178. [[CrossRef](#)]
60. Xiang, S.L.; Huang, J.; Li, L.; Zhang, J.Y.; Jiang, L.; Kuang, X.J.; Su, C.Y. Nanotubular metal-organic frameworks with high porosity based on T-Shaped pyridyl dicarboxylate ligands. *Inorg. Chem.* **2011**, *50*, 1743–1748. [[CrossRef](#)] [[PubMed](#)]
61. Li, L.J.; Tang, S.F.; Wang, C.; Lv, X.X.; Jiang, M.; Wu, H.Z.; Zhao, X.B. High gas storage capacities and stepwise adsorption in a UiO type metal-organic framework incorporating Lewis basic bipyridyl sites. *Chem. Commun.* **2014**, *50*, 2304–2307. [[CrossRef](#)] [[PubMed](#)]
62. Wang, J.; Luo, J.H.; Zhao, J.; Li, D.S.; Li, G.H.; Huo, Q.S.; Liu, Y.L. Assembly of two flexible metal-organic frameworks with stepwise gas adsorption and highly selective CO₂ adsorption. *Cryst. Growth Des.* **2014**, *14*, 2375–2380. [[CrossRef](#)]
63. Li, Q.P.; Du, S.W. A family of 3D lanthanide organic frameworks with tunable luminescence and slow magnetic relaxation. *RSC Adv.* **2015**, *5*, 9898–9903. [[CrossRef](#)]
64. Min, Z.Y.; Singh-Wilmot, M.A.; Cahill, C.L.; Andrews, M.; Taylor, R. Isorecticular lanthanide metal-organic frameworks: Syntheses, structures and photoluminescence of a family of 3D phenylcarboxylates. *Eur. J. Inorg. Chem.* **2012**, 4419–4426. [[CrossRef](#)]
65. Meng, X.X.; Zhang, X.J.; Bing, Y.M.; Xu, N.; Shi, W.; Cheng, P. In situ generation of NiO nanoparticles in a magnetic metal-organic framework exhibiting three-dimensional magnetic ordering. *Inorg. Chem.* **2016**, *55*, 12938–12943. [[CrossRef](#)] [[PubMed](#)]
66. Zhao, J.; Zhu, G.H.; Xie, L.Q.; Wu, Y.S.; Wu, H.L.; Zhou, A.J.; Wu, Z.Y.; Wang, J.; Chen, Y.C.; Tong, M.L. Magnetic and luminescent properties of lanthanide coordination polymers with asymmetric biphenyl-3,2',5'-tricarboxylate. *Dalton Trans.* **2015**, *44*, 14424–14435. [[CrossRef](#)] [[PubMed](#)]
67. Fang, M.; Shi, P.F.; Zhao, B.; Jiang, D.X.; Cheng, P.; Shi, W. A series of 3d-4f heterometallic three-dimensional coordination polymers: Syntheses, structures and magnetic properties. *Dalton Trans.* **2012**, *41*, 6820–6826. [[CrossRef](#)] [[PubMed](#)]
68. Zheng, X.F.; Zhou, L.; Huang, Y.M.; Wang, C.G.; Duan, J.G.; Wen, L.L.; Tian, Z.F.; Li, D.F. A series of metal-organic frameworks based on 5-(4-pyridyl)-isophthalic acid: selective sorption and fluorescence sensing. *J. Mater. Chem. A* **2014**, *2*, 12413–12422. [[CrossRef](#)]
69. Lin, X.P.; Hong, Y.H.; Zhang, C.; Huang, R.Y.; Wang, C.; Lin, W.B. Pre-concentration and energy transfer enable the efficient luminescence sensing of transition metal ions by metal-organic frameworks. *Chem. Commun.* **2015**, *51*, 16996–16999. [[CrossRef](#)] [[PubMed](#)]

